

# EUROPHYSICS LETTERS

OFFPRINT

Vol. 67 • Number 3 • pp. 484–490

**The structure of foam cells: Isotropic Plateau polyhedra**

\* \* \*

S. HILGENFELDT, A. M. KRAYNIK, D. A. REINELT and J. M. SULLIVAN



Published under the scientific responsibility of the  
**EUROPEAN PHYSICAL SOCIETY**  
Incorporating  
JOURNAL DE PHYSIQUE LETTRES • LETTERE AL NUOVO CIMENTO



## The structure of foam cells: Isotropic Plateau polyhedra

S. HILGENFELDT<sup>1</sup>(\*), A. M. KRAYNIK<sup>2</sup>, D. A. REINELT<sup>3</sup> and J. M. SULLIVAN<sup>4,5</sup>

<sup>1</sup> *Applied Physics, University of Twente - P.O. Box 217  
7500 AE Enschede, The Netherlands*

<sup>2</sup> *Sandia National Laboratories, Department 9114 MS0834  
Albuquerque, NM 87185-0834, USA*

<sup>3</sup> *Department of Mathematics, Southern Methodist University  
Dallas, TX 75275-0156, USA*

<sup>4</sup> *Department of Mathematics, University of Illinois - Urbana, IL 61801-2975, USA*

<sup>5</sup> *Institut für Mathematik, Technische Universität Berlin - D-10623 Berlin, Germany*

(received 16 December 2003; accepted in final form 25 May 2004)

PACS. 82.70.Rr – Aerosols and foams.

PACS. 61.43.-j – Disordered solids.

**Abstract.** – A mean-field theory for the geometry and diffusive growth rate of soap bubbles in dry 3D foams is presented. Idealized foam cells called isotropic Plateau polyhedra (IPPs), with  $F$  identical spherical-cap faces, are introduced. The geometric properties (*e.g.*, surface area  $S$ , curvature  $R$ , edge length  $L$ , volume  $V$ ) and growth rate  $\mathcal{G}$  of the cells are obtained as analytical functions of  $F$ , the sole variable. IPPs accurately represent average foam bubble geometry for arbitrary  $F \geq 4$ , even though they are only constructible for  $F = 4, 6, 12$ . While  $R/V^{1/3}$ ,  $L/V^{1/3}$  and  $\mathcal{G}$  exhibit  $F^{1/2}$  behavior, the specific surface area  $S/V^{2/3}$  is virtually independent of  $F$ . The results are contrasted with those for convex isotropic polyhedra with flat faces.

Dry soap foams (with liquid volume fraction  $\ll 1$ ) are space-filling structures composed of polyhedral cells (bubbles) with curved faces. Over short time scales, the bubbles change shape under the influence of surface tension until the total surface area of the foam achieves a local minimum. Over longer times, further area reduction results from gas diffusion between neighboring cells with different internal pressures. Some cells shrink in the process and eventually disappear, increasing the average bubble size. This diffusive coarsening [1] is paradigmatic for other surface-minimizing evolution processes, such as grain growth in polycrystalline metals [2] or domain dynamics in magnetic thin films [3] and lipid monolayers [4].

The statistics and dynamics of foam coarsening are not fully understood, largely because it is hard to quantify the *shape* of 3D cells. A cell of volume  $V$  grows or shrinks [5, 6] as

$$V^{-1/3} \dot{V} = -D V^{-1/3} \int \mathcal{H} \, dA = D \mathcal{G}, \quad (1)$$

where  $D$  is an effective diffusion coefficient [7], and  $\mathcal{G}$  is a dimensionless function of cell shape only, proportional to the mean curvature  $\mathcal{H}$  integrated over the surface. For semi-dilute suspensions where the bubbles are spherical and  $\mathcal{G} = -(48\pi^2)^{1/3}$ , a complete coarsening theory

---

(\*) E-mail: sascha@tn.utwente.nl

is available (*e.g.*, in Ostwald ripening [5]). For ordered foams, such as the Kelvin and Weaire-Phelan structures, it is easy to calculate cell shapes accurately [8], but not for generic (random, disordered) foams, which contain an impressive variety of cells [9, 10]. This letter presents a mean-field theory for the geometry of a class of idealized foam cells, from which  $\mathcal{G}$  and other properties follow. These cells have the simplest possible shapes that satisfy local equilibrium.

A pure mean-field average over all cells in a foam of fixed total volume trivially yields  $\langle \dot{V} \rangle = 0$  in the absence of cell disappearance. Recent experiments [11], simulations, and theory [12] found strong correlations between the coarsening rate of foam cells and the number of faces, naturally dividing the foam into *classes* of  $F$ -faced bubbles. Our goal is to find *representative*  $F$ -hedral foam cells whose shapes can be described analytically, just like the spherical bubbles in Ostwald ripening.

Thermodynamically, random foams are far from equilibrium, prone to effects of jamming and disorder, much like glasses [13]. It is known that in metallic glasses local dodecahedral order competes with long-range disorder [14]. In the same way, we expect foam bubbles to tend toward locally optimal shapes competing with randomness on a global scale.

What are these locally optimal shapes? We argue that bubbles approximate compact, *isotropic* shapes, because i) highly distorted cells with large aspect ratios are energetically unfavorable, as they tend to increase the specific surface area  $S/V^{2/3}$ , and ii) isotropic bubbles are the most probable, in the following sense. During foam generation and evolution, cells explore the space of possible shapes. In a random foam, we can assume, as a first approximation, that all partitions of the surface into  $F$  faces have equal prior probability (mean-field approach). A configurational entropy [15, 16] can then be defined by

$$Q = - \sum_{i=1}^F \omega_i \log \omega_i, \quad \sum_i \omega_i = 1, \quad (2)$$

where  $\omega_i = \Omega_i/4\pi$ , and each face  $i$  on the bubble takes up a solid angle  $\Omega_i$  (as seen from the bubble's center of mass), so that  $\sum \Omega_i = 4\pi$ . It is well known that  $Q$  is maximal when  $\omega_i = 1/F$  for all  $i$ . By a similar argument, as every face is delineated by  $\eta$  edges, we find that the most probable configuration is that of equal edge length, where the vertices are those of a regular polygon. Note that the energy of a *single* foam cell is minimized when  $F-1$  faces are vanishingly small and the last face takes on spherical shape [17]. However, according to formula (2), the probability of such a configuration in a random foam decreases rapidly for large  $F$ .

We therefore propose that representative  $F$ -hedra have  $F$  *identical regular* faces with  $\eta$  vertices *each*;  $\eta = 6 - 12/F$  because foams cells are trivalent (simple) polyhedra. Thus,  $\eta$  is an integer only when  $F = 4, 6$ , or  $12$ <sup>(1)</sup>, and the only physically realizable class representatives have the symmetries of the regular tetrahedron, cube, and pentagonal dodecahedron (fig. 1a). Like every foam cell in 3D, these bubbles must fulfill Plateau's rules [1, 18]: their faces are constant mean-curvature surfaces meeting at dihedral angles of  $120^\circ$ , delineated by edges that meet at the tetrahedral angle  $\arccos(-1/3) \approx 109.47^\circ$ . To emphasize the importance of Plateau's rules, we refer to the representative foam cells as *isotropic Plateau polyhedra* (IPPs).

We now show that all geometric properties of IPPs (referred to as  $P_F$ ) are determined exactly by their symmetry. *A priori*, one could imagine different faces of constant mean curvature, but spatially varying principal curvatures. However, every IPP face can be decomposed into  $2\eta$  triangular symmetry units spanning points at  $A$ ,  $E$ , and  $\mathcal{V}$  in fig. 1b. The edges of this triangle are contained in planes that meet the triangle at constant angles, namely  $\pi/2$  along  $AE$  and  $A\mathcal{V}$  (by symmetry) and  $\pi/3$  along  $E\mathcal{V}$  (by Plateau's rules). The capillary surface

---

<sup>(1)</sup>We shall discuss the non-regular cases  $F = 2, 3, \infty$  later.

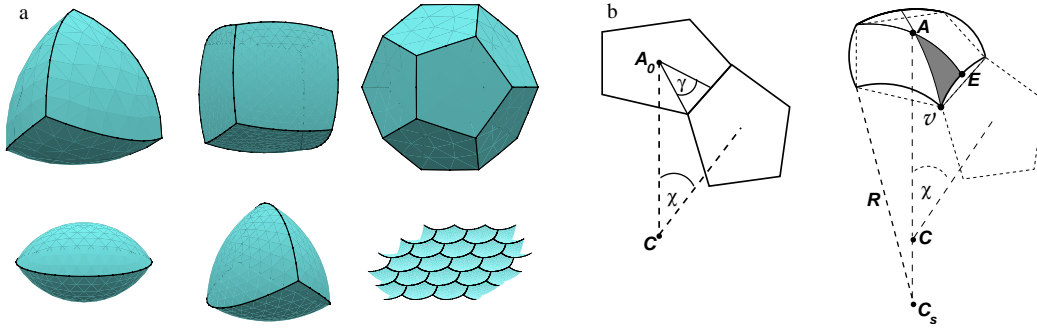


Fig. 1 – (a) Isotropic Plateau polyhedra  $P_4$ ,  $P_6$ ,  $P_{12}$  (top row), the “degenerate” polyhedra  $P_2$ ,  $P_3$ , and a section of the “golf ball”  $P_\infty$  (bottom row). (b) Left: two faces of  $P_{12}^0$ , the flat-faced pentagonal dodecahedron, indicating the angles  $\gamma$  and  $\chi$ . Right: a spherical-cap face with center  $C_s$  and radius  $R$  belonging to  $P_{12}$  has been constructed on one of the flat faces. The elementary symmetry unit of the faces  $AVE$  is shown shaded.

theorems [19, 20] then prove that IPPs with integer  $\eta$  have *spherical-cap faces*, so that their geometric shape is known analytically. This statement is not true for general foam bubbles, and spherical caps had to be taken as an explicit assumption in earlier work [12].

In the following, we derive cell properties by assuming that  $AVE$  is the elementary symmetry unit for arbitrary  $F$  even though this is only true when  $F = 4, 6, 12$ . We interpret our results as approximations to the *statistical, average* properties of  $F$ -faced foam cells in a *random* foam, and show that this approximation works extremely well. Isotropic Plateau polyhedra are not the same as the “ideal average bubbles” discussed by Sire [21]. The latter are semi-regular polyhedra with spherical faces of multiple types; their variability necessitates various closure schemes. More obvious differences exist between the present work and foam models that assume planar [22] or pentagonal faces [23]. Furthermore, the present work goes beyond Hilgenfeldt *et al.* [12] in avoiding any geometric approximations. Equivalent to some of the following formulas were reported by Glicksman [24].

To quantify the geometry of  $P_F$ , consider the analogous convex isotropic polyhedron  $P_F^0$ , which has  $F$  *flat* faces, unit edge length, and center at  $C$ . Figure 1b shows two adjacent faces of  $P_F^0$ . Each face is a regular  $\eta$ -gon and has a fundamental triangle with angle  $\gamma = \pi/\eta$  at the center  $A_0$ . The triangle has side lengths  $\frac{1}{2}$ ,  $\frac{1}{2}/\tan \gamma$  and  $\frac{1}{2}/\sin \gamma$ . Three  $\eta$ -gons form each corner of  $P_F^0$  and determine the angle  $\chi$  between adjacent face normals, given by  $T^2 = 4 \sin^2 \gamma - 1$ , where  $T = \tan(\chi/2)$ . The flat polyhedra only satisfy the Plateau condition when  $\chi = \pi/3$ , which occurs for  $F = F_0^* \approx 13.3973$ , a number well known from other foam theories [25].

To determine the spherical-cap radius  $R$ , notice that two identical spheres intersect at the Plateau dihedral angle when each passes through the other’s center. The intersection is a circle of radius  $r = R\sqrt{3}/2$ ; its curvature as a space curve is  $1/r$ , and, because of the known dihedral angle, its geodesic curvature as a curve on either sphere is  $\kappa_g = 1/2r$ . Consider a typical vertex  $\mathcal{V}$  as shown in fig. 1b, which lies in the plane that contains the face of  $P_F^0$ ; it lies on the sphere of radius  $R$  around  $C_s$ ; and it also lies in the plane through  $C$  and the edge of  $P_F^0$ . These conditions on  $\mathcal{V}$  and the dihedral angle yield

$$R = \frac{3}{2(\sqrt{2} T - \cos \gamma)}, \quad (3)$$

which is positive for  $F < F_0^*$  (indicating convex faces), and negative for  $F > F_0^*$  (concave faces). When  $F = 4$ , the spherical cap has unit radius;  $P_4$  is therefore a Reuleaux tetrahe-

dron [26]. Experiments show that tetrahedral bubbles in real foams have shapes very close to Reuleaux tetrahedra [27], stressing the relevance of the present theory to real systems.

To evaluate the surface area of  $P_F$ , we use the Gauss-Bonnet theorem [28]. For any patch  $\mathcal{D}$  with boundary  $\partial\mathcal{D}$  on a 2D surface,

$$\int_{\mathcal{D}} \mathcal{K} \, dA = 2\pi - \int_{\partial\mathcal{D}} \kappa_g \, ds - \sum_{\nu_i} \phi_i. \quad (4)$$

In our case, the integral of Gaussian curvature  $\mathcal{K} = 1/R^2$  is evaluated over the cap surface, the integral of  $\kappa_g = 1/R\sqrt{3}$  along the edges (circular arcs of unit chord length), and the “turning angles”  $\phi_i$  at each vertex on the boundary (Plateau’s rules require  $\phi_i = \delta \equiv \arccos \frac{1}{3}$ ). The total surface area  $S$  is then

$$S = FR^2 \left( 2\pi - \eta \left( \arcsin \frac{1}{R\sqrt{3}} + \delta \right) \right), \quad (5)$$

while the total edge length  $L$  of  $P_F$ , which has  $3F - 6$  edges, is given by

$$\frac{L}{3(F-2)} = \int_{\partial\mathcal{D}} ds = \sqrt{3} R \arcsin \frac{1}{R\sqrt{3}}. \quad (6)$$

The volume of  $P_F$  is  $V = 2\eta F V_p$ , where  $V_p$  is the volume of the elementary pyramid defined by  $C$  and the fundamental triangle within each face. Choosing  $C$  as origin of a spherical  $r, \theta, \phi$  coordinate system, we find

$$V_p = \frac{1}{3} \int_0^\gamma d\phi \int_0^{\arctan \frac{T}{\cos \phi}} r_{\max}(\theta)^3 \sin \theta \, d\theta, \quad (7)$$

where  $r_{\max} = \frac{R}{2T} (\sqrt{1+T^2} \cos \theta + ((3 + \cos^2 \theta)T^2 - \sin^2 \theta)^{\frac{1}{2}})$  is obtained by using the law of cosines for the triangle shown in fig. 1b. The total volume is

$$V = \frac{\eta FR^3}{72} (2\sqrt{2} + 48\gamma - 57\delta + 33y - \tan y), \quad (8)$$

where  $y = \arcsin(\frac{2}{\sqrt{3}} \cos \gamma)$ . For comparison, the geometric quantities for the convex isotropic polyhedra  $P_F^0$  (cf. [29, 30]) are

$$S_0 = \frac{F\eta}{4} \cot \gamma, \quad L_0 = 3(F-2), \quad V_0 = \frac{F\eta}{24T} \cot^2 \gamma. \quad (9)$$

The characteristic length  $V^{1/3}$  is used to scale all geometric quantities. The sphere is the ultimate surface area minimizer ( $S/V^{2/3} = (36\pi)^{1/3}$ ), so we define a *reduced surface-to-volume ratio*  $\beta = S/(36\pi V^2)^{1/3}$ .

Figure 2a shows that  $\beta$  is a monotonically decreasing function of  $F$  for both types of polyhedra. However, the asymptotic behavior for large  $F$  is surprisingly different. The flat polyhedra approximate a sphere,

$$\beta_0 \approx 1 + 1.0077 F^{-1} + 1.7310 F^{-2}, \quad (10)$$

and  $P_F^0(F \rightarrow \infty)$  is locally equivalent to a plane tiled by flat hexagons. The curved polyhedra tend to a state of larger surface area,

$$\beta \approx \beta_\infty + 0.01743 F^{-1/2} + 0.00228 F^{-1}, \quad (11)$$

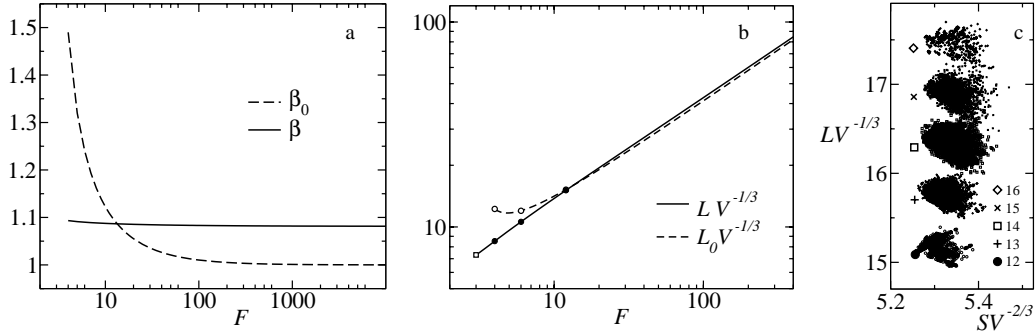


Fig. 2 – (a) Normalized surface area  $\beta$  vs.  $F$  for the isotropic Plateau polyhedra  $P_F$  and the convex isotropic polyhedra  $P_F^0$ , which have flat faces. (b) Non-dimensional edge length  $LV^{-1/3}$  vs.  $F$  for  $P_F$  and  $P_F^0$ . The two curves in both (a) and (b) intersect at  $F = F_0^*$ . (c) Plot of  $LV^{-1/3}$  vs.  $SV^{-2/3}$  for monodisperse foams. Point clouds refer to numerical simulations [10]; polyhedra with the same  $F$  (see legend) cluster in well-separated clouds. Large symbols indicate theoretical values from (11) and (12). Deviations between simulation and theory are typically about 1 – 2% on both axes.

where  $\beta_\infty = 2(5\pi - 12\delta)/\sqrt{3} \approx 1.0813$ . Locally,  $P_F(F \rightarrow \infty)$  is equivalent to a “golf ball” covered by a hexagonal pattern of concave spherical dimples with  $R_\infty = -\sqrt{3}$  (fig. 1a). The specific surface area of IPPs is virtually independent of topology:  $1.0813 \leq \beta \leq 1.0933$  for  $F \geq 4$ , analogous to what is found for 2D foams [31].

The edge length, by contrast, is strongly dependent on topology. Figure 2b shows that the large- $F$  behavior for both types of polyhedra is very similar:

$$\begin{aligned} LV^{-1/3} &\approx \lambda_\infty F^{1/2} + 1.2313 + 2.0455 F^{-1/2}, \\ L_0V_0^{-1/3} &\approx \lambda_\infty^0 F^{1/2} + 2.9184 F^{-1/2}, \end{aligned} \quad (12)$$

where  $\lambda_\infty^0 = 2^{5/6}3^{7/12}\pi^{1/6} \approx 4.0930$  and  $\lambda_\infty = 3 \arcsin(1/3)$   $\lambda_\infty^0 \approx 4.1728$  (the curved edges of the “golf ball” are slightly longer). To excellent accuracy, the edge length of  $P_F$  is proportional to  $F^{1/2}$  over the entire range of  $F$ , but the  $P_F^0$  deviate from power law behavior below  $F_0^*$ , with a local minimum at  $F \approx 4.8663$ .

Figure 2c plots  $LV^{-1/3}$  and  $SV^{-2/3}$  against each other, both from the above theoretical predictions (11), (12) and from simulations of thousands of polyhedra in random monodisperse foams in [10] (point clouds). The predicted, almost constant value of  $SV^{-2/3}$  is both a very good approximation and an approximate lower bound to the actual values of individual bubbles in a random monodisperse foam (fig. 2c). The latter is expected, as disorder leads to distortions from ideal isotropy [10], increasing the surface-to-volume ratio. The edge length  $LV^{-1/3}$ , however, is in very close agreement with the *mean* found in random foam bubbles. This is explained by using the Gauss-Bonnet theorem, written for the whole IPP bubble  $P_F$ :

$$\frac{S}{R^2} + \frac{L}{\sqrt{3}R} = 2\pi F - 6(F - 2)\delta. \quad (13)$$

In monodisperse foams, all bubble faces are very weakly curved ( $R$  is large), so the first (surface) term is much smaller than the second (edge) term. A real foam bubble can be interpreted as a deformation, at fixed  $F$ , of an idealized IPP bubble. Its curvature (and therefore  $R$ ) will increase or decrease from the IPP value, which is compensated by changes in edge length, giving rise to the spread around the mean observed in fig. 2c. By contrast, changing  $S$  cannot compensate for arbitrary changes in curvature because the surface term in (13) is small.

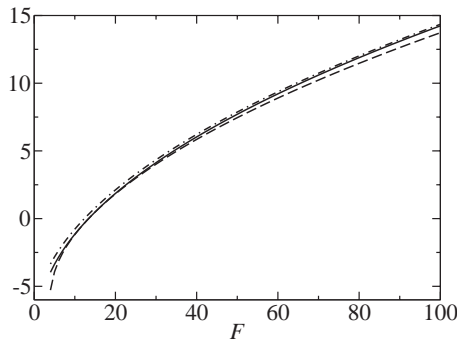


Fig. 3 – Dimensionless growth function  $\mathcal{G}(F)$  from [12] (dashed line), the exact result (14) (solid line), and the leading-order expansion (15) (dot-dashed line).

Recent Surface Evolver simulations of a larger class of quasi-regular bubbles [32] reveal values for  $\beta$  and  $L/V^{1/3}$  very close to the IPP predictions, and show that earlier approximations [12] led to significant discrepancies between theory and simulations for small  $F$ , which are resolved by the present work.

The Surface Evolver was used to calculate  $P_4$ ,  $P_6$ , and  $P_{12}$  (see fig. 1a). Simulations were also performed for  $F = 2$  and 3, where  $\eta$  again is an integer, although bubbles with two or three faces are not conventional foam cells. These degenerate cells are “small inclusions”, sitting in the interior of a larger face ( $F = 2$ ) or on an edge shared by three adjacent faces ( $F = 3$ ). Dihedral and trihedral bubbles have been observed in the laboratory [33], but neither can exist as polyhedra with flat faces. All of the geometric quantities calculated with the Surface Evolver, such as edge length, curvature and area, agree with the analytical solutions except the dihedral bubble. The radius  $R$  according to (3) is a real-valued function for  $F \geq 5/2$  and alternates between real and complex for  $F < 5/2$ ;  $R$  is singular at  $F = 2$  where  $\eta = 0$ .

Our results for bubble geometry apply to diffusive coarsening. From the definition of  $\mathcal{G}$ , we obtain

$$\mathcal{G}(F) = -\frac{S}{R V^{1/3}}. \quad (14)$$

The asymptotic behavior for  $F \rightarrow \infty$  is given by

$$\mathcal{G} \approx 3^{7/12} \left(\frac{\pi}{2}\right)^{1/6} \beta_\infty F^{1/2} - g_1, \quad (15)$$

where  $3^{7/12}(\frac{\pi}{2})^{1/6}\beta_\infty \approx 2.2129$  and  $g_1 \approx 7.7777$  is known analytically. The growth function  $\mathcal{G}(F)$  from (14) and the asymptotic expansion (15) are shown in fig. 3, together with the approximation  $\mathcal{G}_H$  obtained in [12]. The new asymptote is a slightly more faithful (and more uniform) approximation to the exact theory than  $\mathcal{G}_H$ , although the relative error between  $\mathcal{G}$  and  $\mathcal{G}_H$  remains very small throughout the whole range of  $F$  (the error vanishes at  $F = F_0^*$ , where  $\mathcal{G} = \mathcal{G}_H = 0$ ).

To go beyond the present mean-field theory, deviations from the shape of isotropic Plateau polyhedra need to be quantified. One way of doing this was shown in [12]: Using Minkowski’s theorems [34], a distribution of non-isotropic cell shapes can be found and approximations for their growth rates are obtained. Thus, the method developed in [12] remains useful for describing disordered foams, until improved upon by a rigorous extension of the present work.

\*\*\*

The main analytical results of this work were obtained while the authors attended a workshop on “Foams and Minimal Surfaces” at the Isaac Newton Institute for Mathematical Sci-



ences, Cambridge, UK, from July 29 to August 23, 2002. Sandia is a multiprogram laboratory operated by Sandia Corporation, a Lockheed Martin Company, for the U.S. Department of Energy's National Nuclear Security Administration under contract #DE-AC04-94AL85000.

## REFERENCES

- [1] WEAIRE D. and HUTZLER S., *The Physics of Foams* (Oxford University Press, Oxford) 2000.
- [2] SMITH C. S., in *Metal Interfaces*, edited by HERRING C. (American Society for Metals, Cleveland) 1952.
- [3] DE ALBUQUERQUE M. P. and MOLHO P., *J. Magn. & Magn. Mater.*, **113** (1992) 132.
- [4] BERGE B., SIMON A. J. and LIBCHABER A., *Phys. Rev. A*, **41** (1990) 6893.
- [5] MULLINS W. W., *J. Appl. Phys.*, **59** (1986) 1341.
- [6] GLAZIER J. A., *Phys. Rev. Lett.*, **70** (1993) 2170.
- [7] HILGENFELDT S., KOEHLER S. A. and STONE H. A., *Phys. Rev. Lett.*, **86** (2001) 4704.
- [8] WEAIRE D. and PHELAN R., *Nature*, **367** (1994) 123; WEAIRE D. (Editor), *The Kelvin Problem* (Taylor & Francis, London) 1996.
- [9] MATZKE E., *Am. J. Bot.*, **33** (1946) 58.
- [10] KRAYNIK A. M., REINELT D. A. and VAN SWOL F., *Phys. Rev. E*, **67** (2003) 031403.
- [11] MONNEREAU C. and VIGNES-ADLER M., *Phys. Rev. Lett.*, **80** (1998) 5228.
- [12] HILGENFELDT S., KRAYNIK A., KOEHLER S. A. and STONE H. A., *Phys. Rev. Lett.*, **86** (2001) 2685.
- [13] LIU A. J. and NAGEL S. R., *Nature*, **396** (1998) 21.
- [14] STEINHARDT P. J., NELSON D. R. and RONCHETTI M., *Phys. Rev. Lett.*, **47** (1981) 1297.
- [15] ELLIS R. S. (Editor), *Entropy, Large Deviations, and Statistical Mechanics* (Springer, New York) 1985.
- [16] RIVIER N., *Philos. Mag. B*, **52** (1985) 795.
- [17] BRAKKE K. A., private communication (2002).
- [18] PLATEAU J. A. F., *Statique expérimentale et théorique des liquides soumis aux seules forces moléculaires* (Gauthier-Villars, Trubner et cie, Paris) 1873.
- [19] CHOE J., *Math. Ann.*, **323** (2002) 143.
- [20] FINN R. and MCCUAN J., *Math. Nachr.*, **209** (2000) 115.
- [21] SIRE C., *Phys. Rev. Lett.*, **72** (1994) 420.
- [22] FORTES M. A., *J. Mat. Sci.*, **21** (1986) 2509.
- [23] MULLINS W. W., *Acta Metall.*, **37** (1989) 2979.
- [24] GLICKSMAN M. E., *Average  $N$ -hedra as a basis for grain shape*, submitted to *Interface Sci.* (2004).
- [25] RIVIER N., *J. Phys. (Paris), Coll. C9*, **43** (1982) 91; KUSNER R., *Proc. R. Soc. London, Ser. A*, **439** (1992) 683.
- [26] WEISSTEIN E. W., *Eric Weisstein's World of Mathematics*, <http://mathworld.wolfram.com/ReuleauxTetrahedron.html>.
- [27] VAN DOORNUM A. and HILGENFELDT S., *Foam tetrahedra: Isotropic bubbles as a tool for in situ film thickness measurements*, submitted to *Phys. Rev. Lett.* (2003).
- [28] MILLMAN R. S. and PARKER G. D. (Editors), *Elements of Differential Geometry* (Prentice-Hall, Englewood Cliffs) 1977.
- [29] ZWILLINGER D. (Editor), *Standard Mathematical Tables and Formulae* (CRC Press, Boca Raton) 1996.
- [30] COX S. J. and FORTES M. A., *Philos. Mag. Lett.*, **83** (2003) 281.
- [31] GRANER F., JIANG Y., JANIAUD E. and FLAMENT C., *Phys. Rev. E*, **63** (2000) 011402.
- [32] COX S. J. and GRANER F., *Three-dimensional bubble clusters: shape, packing and growth-rate*, preprint (2003).
- [33] HILGENFELDT S., unpublished data.
- [34] MINKOWSKI H., *Math. Ann.*, **57** (1903) 447.